

# Accurate Molecular Structures of 16-Electron Rhodium Hydrido Boryl Complexes: Low-Temperature Single-Crystal X-ray and Neutron Diffraction and Computational Studies of $[(\text{PR}_3)_2\text{RhHCl}(\text{Boryl})]$ (Boryl = Bpin, Bcat)

Wai Han Lam,<sup>†</sup> Shigeru Shimada,<sup>‡,§</sup> Andrei S. Batsanov,<sup>‡</sup> Zhenyang Lin,<sup>\*,†</sup> Todd B. Marder,<sup>\*,‡</sup> John A. Cowan,<sup>‡,||</sup> Judith A. K. Howard,<sup>‡</sup> Sax A. Mason,<sup>||</sup> and Garry J. McIntyre<sup>||</sup>

Department of Chemistry, Hong Kong University of Science and Technology, Clear Water Bay, Kowloon, Hong Kong, People's Republic of China, Department of Chemistry, University of Durham, South Road, Durham DH1 3LE, U.K., National Institute of Advanced Industrial Science and Technology (AIST), Tsukuba Central 5, 1-1-1 Higashi, Tsukuba, Ibaraki 305-8565, Japan, and Institut Laue Langevin, 6 Rue Jules Horowitz, BP 156, 38042 Grenoble CEDEX 9, France

Received June 5, 2003

Rhodium hydrido boryl complexes of the form  $[(\text{PR}_3)_2\text{RhHCl}\{\text{B}(\text{OR})_2\}]$  are key first intermediates in several Rh-catalyzed borylation processes. Previous theoretical studies have examined model compounds, e.g with  $\text{PH}_3$  and  $\text{BH}_2$  or  $\text{B}(\text{OH})_2$  groups, and there were little structural data available for this class of compounds to compare with the calculated structures. This paper reports the results of single-crystal X-ray (at 120 K) and neutron (at 20 K) diffraction studies on two such complexes, namely  $[(\text{P}^i\text{Pr}_3)_2\text{RhHCl}(\text{Bpin})]$  (**3Bpin**) and  $[(\text{P}^i\text{Pr}_3)_2\text{RhHCl}(\text{Bcat})]$  (**3Bcat**) (pin =  $\text{OCMe}_2\text{CMe}_2\text{O}$ ; cat = 1,2- $\text{O}_2\text{C}_6\text{H}_4$ ), providing the first accurate location of the hydride ligands in a hydrido boryl complex. The orientations of the boryl ligands with respect to the equatorial plane of a distorted-trigonal-bipyramidal (DTBP) structure differs for the two compounds (Bpin lies nearly perpendicular to this plane, whereas Bcat is roughly coplanar with it), and the Cl–Rh–B angles are also very different, being 117.73(4) and 137.87(5)° (X-ray data), respectively, for **3Bpin** and **3Bcat**. The Rh–H distances are 1.571(5) and 1.531(11) Å, and the B–Rh–H angles are only 67.8(2) and 68.5(4)°, leading to B···H separations of 2.013(5) and 2.004(10) Å (neutron data) in the two compounds. Thus, these are best described as  $\text{Rh}^{\text{III}}$  hydrido boryl rather than  $\text{Rh}^{\text{I}}$   $\sigma$ -borane ( $\sigma\text{-HB}(\text{OR})_2$ ) complexes, although there is a modest residual B···H interaction in both compounds. DFT calculations on model compounds employing  $\text{PH}_3$  and  $\text{PMe}_3$ , as well as on **3Bpin** and **3Bcat**, incorporating the actual  $\text{P}^i\text{Pr}_3$ , Bpin, and Bcat ligands allowed a detailed examination of the factors influencing structure and bonding in these compounds as well as a direct comparison of theory and experiment. The perpendicular arrangement of the boryl ligand is calculated to be favored for all cases except for **3Bcat** (i.e.  $\text{P}^i\text{Pr}_3$ ; Bcat), for which steric constraints appear to be responsible for a small preference for the coplanar form. This and the calculated geometric parameters are in good agreement with the experimental structures. The theoretical study confirms the residual B···H interaction in both **3Bpin** and **3Bcat**, indicating that B–H interaction can occur through both the “empty”  $\text{BO}_2$   $p(\pi^*)$  and  $\text{BO}_2$   $\sigma^*$  orbitals, which are mutually perpendicular. The latter interaction has not been addressed in previous studies. The degree of oxidative addition of the B–H bond depends on the electron-donating properties of the phosphine ligand and also on the nature and orientation of the boryl ligand. Thus, the balance of factors involved in the determination of the structure of these species is quite subtle, and care needs to be taken in using models in the analysis of these systems.

## Introduction

The transition-metal boryl complexes<sup>1</sup>  $\text{L}_n\text{M}-\text{BX}_2$ , first reported in 1963,<sup>2</sup> have attracted particular atten-

tion since the 1985 discovery<sup>3a</sup> of rhodium-catalyzed hydroboration of olefins using HBcat (cat = 1,2- $\text{O}_2\text{C}_6\text{H}_4$ ),<sup>3</sup> as they are postulated intermediates in this process, which can provide regio-, diastereo-, and chemoselectivities often quite different from those of the uncatalyzed process. More recently, metal boryl complexes have been shown to be involved in catalyzed diborations and related B–X addition reactions<sup>4</sup> and, most remarkably, in the catalyzed dehydrogenative

\* To whom correspondence should be addressed. E-mail: chzlin@ust.hk (Z.L.); todd.marder@durham.ac.uk (T.B.M.).

<sup>†</sup> Hong Kong University of Science and Technology.

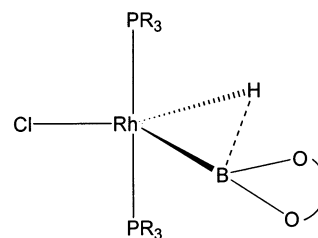
<sup>‡</sup> University of Durham.

<sup>§</sup> National Institute of Advanced Industrial Science and Technology (AIST).

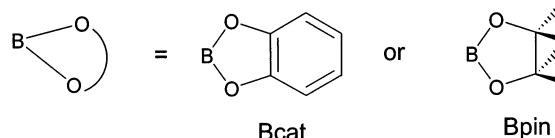
<sup>||</sup> Institut Laue Langevin.

borylation of C–H bonds in alkanes, arenes, and alkenes.<sup>1a,5–8</sup>

The most widely employed catalyst precursors for alkene hydroboration are rhodium phosphine complexes<sup>9</sup> such as [(PPh<sub>3</sub>)<sub>3</sub>RhCl], and the most common boron reagents are those containing B–O bonds, such as HBcat. Notwithstanding several high-level theoretical studies of catalyzed olefin hydroboration employing model ligands (e.g. PH<sub>3</sub>, B(OH)<sub>2</sub>),<sup>10</sup> its mechanism, for example, associative or dissociative with regard to phosphine and H migration or boryl migration to coordinated alkene, remains disputed. It would appear from experimental data that, at least for the latter step, both processes are possible. Whatever ambiguities remain, it is clear that the first step in the catalytic cycle is the (oxidative) addition of H–B(OR')<sub>2</sub> to the Rh

Chart 1. <sup>a</sup>

- 1, R = H
- 2, R = Me
- 3, R = <sup>i</sup>Pr
- 4, R = Ph



<sup>a</sup> The notation of *n*boryl is used to distinguish the different phosphine (**1** = PH<sub>3</sub>, **2** = PMe<sub>3</sub>, **3** = P<sup>i</sup>Pr<sub>3</sub>, **4** = PPh<sub>3</sub>) and boryl ligands (**Bcat** and **Bpin**; cat = 1,2-O<sub>2</sub>C<sub>6</sub>H<sub>4</sub>, pin = OCMe<sub>2</sub>CM<sub>2</sub>O) discussed in this paper. For example, **1Bcat** is (PH<sub>3</sub>)<sub>2</sub>RhHClBcat, while **2Bpin** denotes (PMe<sub>3</sub>)<sub>2</sub>RhHClBpin.

center, yielding a 5-coordinate, 16-electron “hydrido-boryl” complex, i.e., [(PR<sub>3</sub>)<sub>2</sub>RhClH{B(OR')<sub>2</sub>}] (**1–4**; Chart 1).<sup>3a,9,11</sup> The same type of initial intermediate was observed for the rhodium-catalyzed borylation<sup>7</sup> of aromatic and benzylic C–H bonds using [(P<sup>i</sup>Pr<sub>3</sub>)<sub>2</sub>Rh(N<sub>2</sub>)Cl] and HBpin. Knowledge of the structure and bonding in [(PR<sub>3</sub>)<sub>2</sub>RhClH{B(OR')<sub>2</sub>}] complexes is necessary in order to develop a clearer understanding of their reactivity and the mechanisms of the catalytic reactions.

In fact, although the complex [(PPh<sub>3</sub>)<sub>2</sub>RhClH(Bcat)] (**4Bcat**) has been known<sup>11a</sup> since 1975, it has proved impossible to date to obtain single crystals suitable for X-ray diffraction experiments. In contrast, it was possible to obtain preliminary X-ray diffraction data<sup>11b</sup> on the P<sup>i</sup>Pr<sub>3</sub> analogue [(P<sup>i</sup>Pr<sub>3</sub>)<sub>2</sub>RhClH(Bcat)] (**3Bcat**) in 1991, although the hydride ligand could not be located. In conjunction with our communication of catalyzed C–H borylation, we recently reported<sup>7</sup> the X-ray structure of [(P<sup>i</sup>Pr<sub>3</sub>)<sub>2</sub>RhClH(Bpin)] (**3Bpin**), which showed large differences in terms of the rotational orientation of the boryl moiety and the Cl–Rh–B angle when compared with the Bcat compound. In addition, the X-ray diffraction study indicated a rather small B–Rh–H angle of 70.0(8)° and consequent relatively short B···H separation of 2.02(3) Å.

It is noteworthy that oxidative addition of the B–H bond to the metal center is characteristic of the *late* transition metals, e.g. Ir,<sup>6,12</sup> while the early and middle transition metals can form a variety of products,<sup>1b</sup> varying from genuine hydrido boryl complexes (type A,

(1) For recent reviews see: (a) Hartwig, J. F.; Waltz, K. M.; Muhoro, C. N.; He, X.; Eisenstein, O.; Bosque, R.; Maseras, F. In *Advances of Boron Chemistry*; Siebert, W., Ed.; Spec. Publ. No. 201, Royal Society of Chemistry: Cambridge, U.K., 1997; pp 373–396. (b) Wadepohl, H. *Angew. Chem., Int. Ed. Engl.* **1997**, *36*, 2441–2444. (c) Irvine, G. J.; Lesley, M. J. G.; Marder, T. B.; Norman, N. C.; Rice, C. R.; Robins, E. G.; Roper, W. R.; Whittell, G. R.; Wright, L. J. *Chem. Rev.* **1998**, *98*, 2685–2722. (d) Braunschweig, H. *Angew. Chem., Int. Ed.* **1998**, *37*, 1786–1801. (e) Smith, M. R., III. *Prog. Inorg. Chem.* **1999**, *48*, 505–567. (f) Braunschweig, H.; Colling, M. *Coord. Chem. Rev.* **2001**, *223*, 1–51.

(2) Nöth, H.; Schmid, G. *Angew. Chem., Int. Ed. Engl.* **1963**, *2*, 623–624.

(3) (a) Männing, D.; Nöth, H. *Angew. Chem., Int. Ed. Engl.* **1985**, *24*, 878–879. For reviews see: (b) Burgess, K.; Ohlmeyer, M. J. *Chem. Rev.* **1991**, *91*, 1179–1191. (c) Burgess, K.; van der Donk, W. A. In *Encyclopedia of Inorganic Chemistry*; King, R. B., Ed.; Wiley: Chichester, U.K., 1994; Vol. 3, p 1420. (d) Fu, G. C.; Evans, D. A.; Muci, A. R. In *Advances in Catalytic Processes*; Doyle, M. P., Ed.; JAI: Greenwich, CT, 1995; p 95. (e) Beletskaya, I.; Pelter, A. *Tetrahedron* **1997**, *53*, 4957–5026.

(4) For recent reviews, see: (a) Marder, T. B.; Norman, N. C. *Top. Catal.* **1998**, *5*, 63–73. (b) Ishiyama, T.; Miyaura, N. *J. Synth. Org. Chem. Jpn.* **1999**, *57*, 503–511. (c) Ishiyama, T.; Miyaura, N. *J. Organomet. Chem.* **2000**, *611*, 392–402.

(5) (a) Iverson, C. N.; Smith, M. R., III. *J. Am. Chem. Soc.* **1999**, *121*, 7696–7697. (b) Waltz, K. M.; Hartwig, J. F. *J. Am. Chem. Soc.* **2000**, *122*, 11358–11369. (c) Chen, H.; Schlecht, S.; Semple, T. C.; Hartwig, J. F. *Science* **2000**, *287*, 1995–1997. (d) Cho, J.-Y.; Iverson, C. N.; Smith, M. R., III. *J. Am. Chem. Soc.* **2000**, *122*, 12868–12869. (e) Tse, M. K.; Cho, J.-Y.; Smith, M. R., III. *Org. Lett.* **2001**, *3*, 2831–2833. (f) Ishiyama, T.; Ishida, K.; Takagi, J.; Miyaura, N. *Chem. Lett.* **2001**, 1082–1083. (g) Cho, J.-Y.; Tse, M. K.; Holmes, D.; Maleczka, R. E., Jr.; Smith, M. R., III. *Science* **2002**, *295*, 305–308. (h) Ishiyama, T.; Tagaki, J.; Ishida, K.; Miyaura, N.; Anastasi, N. R.; Hartwig, J. F. *J. Am. Chem. Soc.* **2002**, *124*, 390–391. (i) Kondo, Y.; Garica-Cuadrado, D.; Hartwig, J. F.; Boen, N. K.; Wagner, N. L.; Hillmyer, M. A. *J. Am. Chem. Soc.* **2002**, *124*, 1164–1165. (j) Takagi, J.; Sato, K.; Hartwig, J. F.; Ishiyama, T.; Miyaura, N. *Tetrahedron Lett.* **2002**, *43*, 5649–5651. (k) Ishiyama, T.; Takagi, J.; Hartwig, J. F.; Miyaura, N. *Angew. Chem., Int. Ed.* **2002**, *41*, 3056–3058. (l) Wan, X.; Wang, X.; Luo, Y.; Takami, S.; Kubo, M.; Miyamoto, A. *Organometallics* **2002**, *21*, 3703–3708. (m) See also: Webster, C. E.; Fan, Y.; Hall, M. B.; Kunz, D.; Hartwig, J. F. *J. Am. Chem. Soc.* **2003**, *125*, 858–859. (n) Lam, W. H.; Lin, Z. Y. *Organometallics* **2003**, *22*, 473–480. (o) For a review, see: Ishiyama, T.; Miyaura, N. *J. Organomet. Chem.* **2003**, *680*, 3–11.

(6) Baker, R. T.; Ovenall, D. W.; Calabrese, J. C.; Westcott, S. A.; Taylor, N. J.; Williams, I. D.; Marder, T. B. *J. Am. Chem. Soc.* **1990**, *112*, 9399–9400.

(7) Shimada, S.; Batsanov, A. S.; Howard, J. A. K.; Marder, T. B. *Angew. Chem., Int. Ed.* **2001**, *40*, 2168–2171.

(8) Coapes, R. B.; Souza, F. E. S.; Thomas, R. L.; Hall, J. J.; Marder, T. B. *Chem. Commun.* **2003**, 614–615 and references therein.

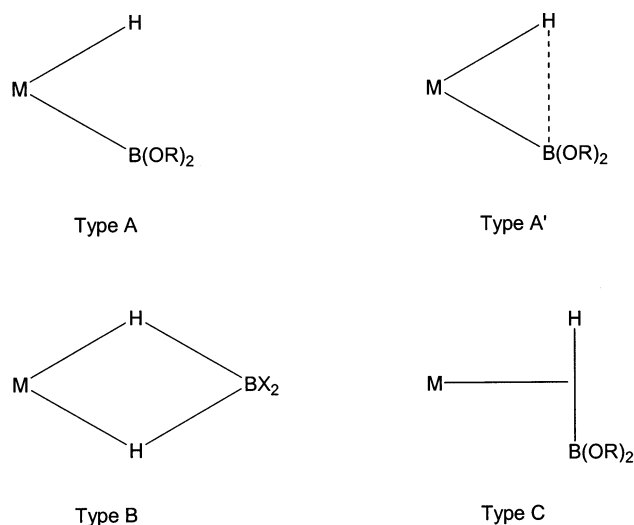
(9) (a) Evans, D. A.; Fu, G. C. *J. Org. Chem.* **1990**, *55*, 2280–2282. (b) Burgess, K.; van der Donk, W. A.; Kook, A. M. *J. Org. Chem.* **1991**, *56*, 2949–2951. (c) Evans, D. A.; Fu, G. C.; Anderson, B. A. *J. Am. Chem. Soc.* **1992**, *114*, 6679–6685. (d) Burgess, K.; van der Donk, W. A.; Westcott, S. A.; Marder, T. B.; Baker, R. T.; Calabrese, J. C. *J. Am. Chem. Soc.* **1992**, *114*, 9350–9359 and references therein.

(10) (a) Musaev, D. G.; Mebel, A. M.; Morokuma, K. *J. Am. Chem. Soc.* **1994**, *116*, 10693–10702. (b) Dorigo, A. E.; Schleyer, P. v. R. *Angew. Chem., Int. Ed. Engl.* **1995**, *34*, 115–118. (c) Widauer, C.; Grützmacher, H.; Ziegler, T. *Organometallics* **2000**, *19*, 2097–2107. For a review, see: (d) Huang, X.; Lin, Z. Y. In *Computational Modeling of Homogeneous Catalysis*; Maseras, F., Lledos, A., Eds.; Kluwer Academic: Amsterdam, 2002; pp 189–212.

(11) (a) Kono, H.; Ito, K.; Nagai, Y. *Chem. Lett.* **1975**, 1095–1096. (b) Westcott, S. A.; Taylor, N. J.; Marder, T. B.; Baker, R. T.; Jones, N. J.; Calabrese, J. C. *J. Chem. Soc., Chem. Commun.* **1991**, 304–305.

(12) (a) Knorr, J. R.; Merola, J. S.; *Organometallics* **1990**, *9*, 3008–3010. (b) Westcott, S. A.; Marder, T. B.; Baker, R. T.; Calabrese, J. C. *Can. J. Chem.* **1993**, *71*, 930–936. (c) Kawamura, K.; Hartwig, J. F. *J. Am. Chem. Soc.* **2001**, *123*, 8422–8423.

Chart 2

Table 1. Calculated Bond Distances (Å) and Angles (deg) in [(PH<sub>3</sub>)<sub>2</sub>RhHCl(X)] Complexes

	MP2 <sup>10b</sup> X = BH <sub>2</sub>	MP2 <sup>10a</sup>		DFT <sup>10c</sup>	
		X = B(OH) <sub>2</sub>	X = BO(CH <sub>2</sub> ) <sub>3</sub> O	X = B(OH) <sub>2</sub>	X = BOCH=CHO
Rh–P	2.368	2.369	2.400	~2.320	~2.320
Rh–Cl	not given	2.448	2.487	2.395	2.392
Rh–B	1.914	2.056	2.050	2.072	2.050
Rh–H	1.522	1.583	1.609	1.641	1.656
B···H(1)	2.145	1.995	2.155	1.495	1.443
Cl–Rh–B	not given	147.2	124.0	146.5	149.0
Cl–Rh–H	not given	147.7	165.0	167.8	166.8
B–Rh–H	not given	65.1	71.0	45.7	44.2

Chart 2) of Ta<sup>13</sup> and W,<sup>14</sup> through hydridoborates (type B) of Ti,<sup>15</sup> Nb,<sup>16</sup> Mo,<sup>17</sup> Re,<sup>18</sup> and Ru,<sup>19</sup> to “side-on”  $\eta^2$ -coordination of a B–H bond in H–BX<sub>2</sub>, in so-called  $\sigma$ -borane complexes (type C) of Ti,<sup>20</sup> Mn,<sup>21</sup> and Ru.<sup>19</sup> The last group is characterized by short B···H distances of 1.24(2)–1.35(3) Å, as determined by X-ray diffraction studies. The question arises as to whether there may be stable structures which are intermediate between types A and C, such as type A’.

Previous ab initio calculations<sup>10</sup> on model compounds, such as [(PH<sub>3</sub>)<sub>2</sub>RhHCl{B(OH)<sub>2</sub>}] and even [(PH<sub>3</sub>)<sub>2</sub>RhHCl(BH<sub>2</sub>)], predicted a substantial degree of three-center Rh/H/B bonding (Chart 2 and Table 1), with B···H distances varying from 1.44 to 2.16 Å. Thus, there is some discrepancy as to whether the first intermediate

(13) Lantero, D. R.; Motry, D. H.; Ward, D. L.; Smith, M. R., III. *J. Am. Chem. Soc.* **1994**, *116*, 10811–10812.

(14) Hartwig, J. F.; He, X. *Organometallics* **1996**, *15*, 5350–5358.

(15) (a) Douthwaite, R. E. *Polyhedron* **2000**, *19*, 1579–1583. (b) For one of the few neutron diffraction studies of a B–H–M interaction, see: Ho, N. N.; Bau, R.; Plecnik, C.; Shore, S. G.; Wang, X.; Schultz, A. J. *J. Organomet. Chem.* **2002**, *654*, 216–220.

(16) Hartwig, J. F.; De Gala, S. R. *J. Am. Chem. Soc.* **1994**, *116*, 3661–3662.

(17) Hascall, T.; Bridgewater, B. M.; Parkin, G. *Polyhedron* **2000**, *19*, 1063–1066.

(18) Jia, G.; Lough, A. L.; Morris, R. H. *J. Organomet. Chem.* **1993**, *461*, 147–156.

(19) Montiel-Palma, V.; Lumbierres, M.; Donnadiu, B.; Sabo-Etienne, S.; Chaudret, B. *J. Am. Chem. Soc.* **2002**, *124*, 5624–5625.

(20) (a) Hartwig, J. F.; Muhoro, C. N.; He, X. *J. Am. Chem. Soc.* **1996**, *118*, 10936–10937. (b) Muhoro, C. N.; Hartwig, J. F. *Angew. Chem., Int. Ed. Engl.* **1997**, *36*, 1510–1512. (c) Muhoro, C. N.; He, X.; Hartwig, J. F. *J. Am. Chem. Soc.* **1999**, *121*, 5033–5046. (d) Lam, W. H.; Lin, Z. Y.; *Organometallics* **2000**, *19*, 2625–2628.

(21) Schlecht, S.; Hartwig, J. F. *J. Am. Chem. Soc.* **2000**, *122*, 9435–9442.

in catalysis is a  $\sigma$ -borane complex, a hydrido boryl complex, or something in between. In other words, even the formal oxidation state of the rhodium in this species is a subject of debate. It is also worth noting that the Cl–Rh–B angle in most cases was calculated to be ca. 147°, but in one case, using [(PH<sub>3</sub>)<sub>2</sub>RhHCl{B(OCH<sub>2</sub>CH<sub>2</sub>CH<sub>2</sub>O)}], the angle was calculated to be much smaller at 124°. In all cases, however, the boryl ligand was found to lie perpendicular to the equatorial plane of the distorted trigonal bipyramid.

Clearly, a better understanding of the bonding and reactivity of transition-metal hydrido boryl complexes requires accurate structural data, but in fact such data are not abundant. Location of hydrogens in the vicinity of heavy atoms by means of X-ray diffraction is not very accurate in principle, and to our knowledge, no complex of this type has been studied by neutron diffraction, which gives the most precise hydrogen positions. We report herein the results of single-crystal X-ray diffraction experiments, at 120 K, and neutron diffraction experiments, at 20 K, for the two compounds **3Bcat** and **3Bpin**, along with a detailed theoretical study of the structures and bonding in these systems and in their PH<sub>3</sub> (**1**) and PMe<sub>3</sub> (**2**) model analogues. Importantly, in the theoretical study, we examined not only the model species but also those containing the real ligands Bcat, Bpin, and P<sup>i</sup>Pr<sub>3</sub>, for which accurate experimental structural data were obtained.

## Results and Discussion

**Background.** For five-coordinate, d<sup>6</sup>-metal complexes in the singlet state, a degeneracy would exist in a perfect trigonal bipyramid. Thus, a Jahn–Teller distortion leads toward either a square-based pyramid (SP) or a distorted trigonal bipyramid (DTBP) with a Y configuration of equatorial ligands: i.e., with one equatorial angle narrowed to  $\leq 80^\circ$ .<sup>22</sup> Note that the Y-shaped distortion is strictly a function of stabilizing the metal  $d(x^2 - y^2)$  orbital with respect to  $d(xy)$  and has nothing to do inherently with any ligand–ligand interactions. For example, such a distortion exists<sup>23</sup> in compounds of the general form [(PR<sub>3</sub>)<sub>2</sub>IrCl(L)(L’)], where L, L’ = alkyl or L = H, L’ = C<sub>5</sub>H<sub>6</sub>. The Y-shaped DTBP structure is stabilized by a ligand with poor  $\sigma$ -donor but good  $\pi$ -donor properties, such as Cl, which would occupy the position opposite to the acute angle. In contrast, good  $\sigma$ -donor/ $\pi$ -acceptor type ligands stabilize the SP configuration and take the apical position therein. Rhodium bis(boryl) complexes such as [(PPh<sub>3</sub>)<sub>2</sub>RhCl(Bcat)<sub>2</sub>] can be viewed either as a distorted version of the SP structure, in which the extremely strong  $\sigma$ -donor Bcat ligands are trans to Cl and to the vacant site, respectively, or as a Y-shaped DTBP, as the actual structures in the solid state are about midway between the two limiting

(22) (a) Rachidi, I. E.-I.; Eisenstein, O.; Jean, Y. *New J. Chem.* **1990**, *14*, 671–677. (b) Riehl, J.-F.; Jean, Y.; Eisenstein, O.; Pélissier, M. *Organometallics* **1992**, *11*, 729–737. (c) Olivani, M.; Eisenstein, O.; Caulton, K. G. *Organometallics* **1997**, *16*, 2227–2229. See also: (d) Daniel, C.; Koga, N.; Han, J.; Fu, X. Y.; Morokuma, K. *J. Am. Chem. Soc.* **1988**, *110*, 3773–3787.

(23) (a) Werner, H.; Hohn, A.; Dziallas, M. *Angew. Chem., Int. Ed. Engl.* **1986**, *25*, 1090–1092. (b) Fryzuk, M. D.; MacNeil, P. A.; Ball, R. G. *J. Am. Chem. Soc.* **1986**, *108*, 6414–6416. (c) Fryzuk, M. D.; MacNeil, P. A.; Massey, R. L.; Ball, R. G. *J. Organomet. Chem.* **1989**, *328*, 231–247.

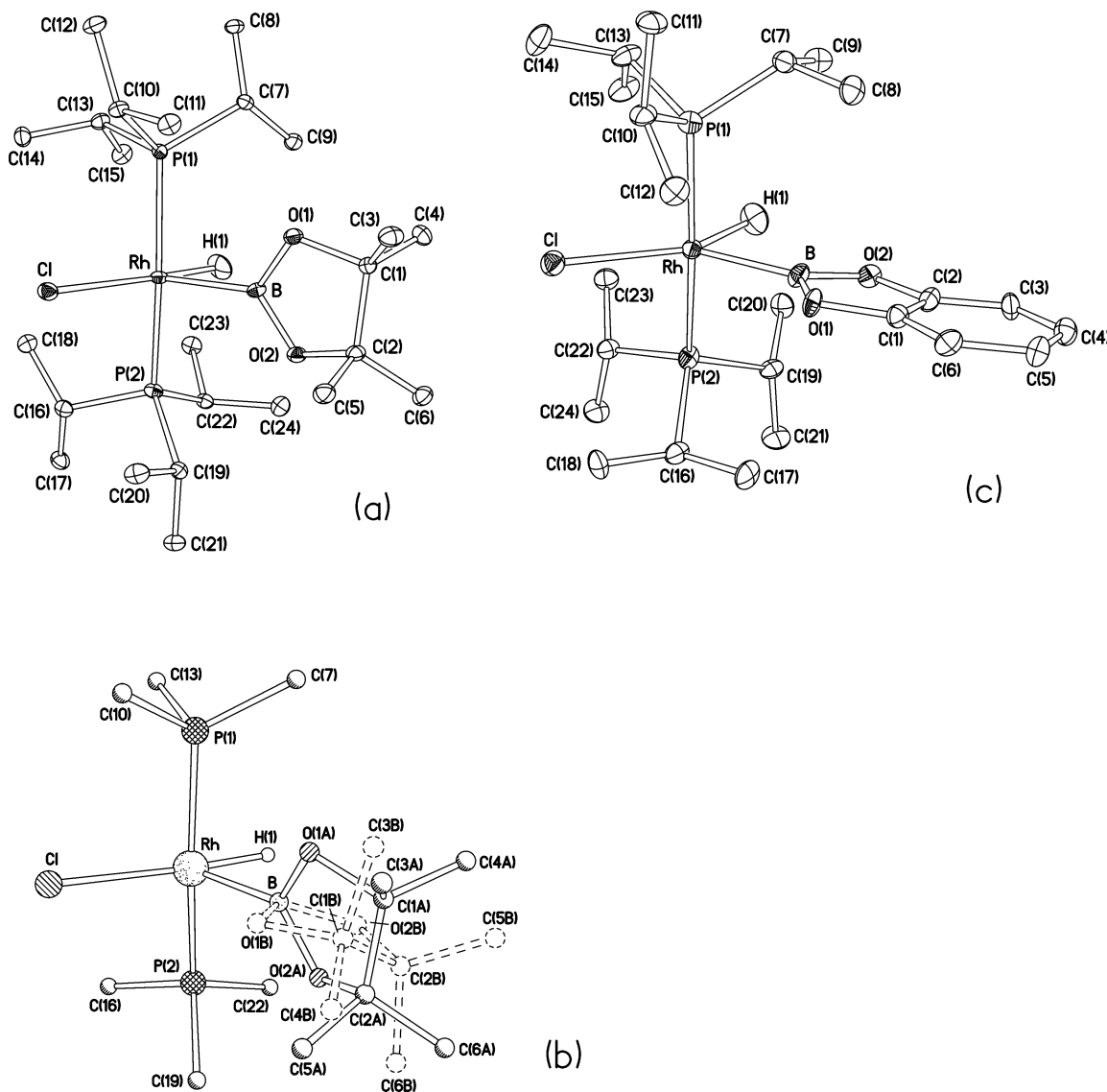


**Figure 1.** Molecular structure of **3Bpin** (a) and **3Bcat** (c) at 20 K from neutron diffraction data and the disorder in **3Bpin** (b) at 120 K from X-ray diffraction data. Thermal ellipsoids are drawn at the 50% probability level. H atoms, except H(1), and the isopropyl methyl groups in (b) are omitted for clarity.

descriptions.<sup>24</sup> The title complexes contain both a  $\pi$ -donating ligand, Cl, and good  $\sigma$ -donors, i.e., boryl and hydride. Thus, both structural types are feasible. In addition, there is a question of whether any B...H interactions affect the structural preference. Finally, the character of the metal–boron bond in boryls is also flexible, affected by competition between the metal d orbitals and the lone pairs or filled  $p\pi$  orbitals of the substituents for the empty p orbital of B.<sup>1,16,25</sup>

**Molecular Structures of 3Bpin and 3Bcat by Single-Crystal X-ray and Neutron Diffraction.** The complex **3Bpin** (Figure 1a,b; Table 2) is only the seventh structurally characterized transition-metal compound with a Bpin moiety, the earlier data comprising one Pt<sup>26</sup> and three Ir<sup>5h,12c</sup> boryls, one pinacolborane B–H  $\sigma$ -complex of Mn,<sup>21</sup> and an Ru complex<sup>19</sup> which contains both  $\sigma$ -H–Bpin and bidentate H<sub>2</sub>Bpin moieties.

In the structure of **3Bpin**, the Rh, P(1), P(2), Cl, and H(1) atoms are almost coplanar with an average deviation of 0.1 Å; therefore, the coordination environment around the Rh can be described as a highly distorted square pyramid (SP) with the boryl ligand occupying the apical position, as was expected theoretically<sup>22</sup> (vide supra), since the boryl ligand can be described as a pseudo-carbene, acting as a very strong  $\sigma$ -donor (B→Rh)

(25) (a) Hartwig, J. F.; Huber, S. *J. Am. Chem. Soc.* **1993**, *115*, 4908–4909. (b) Braunschweig, H.; Ganter, B.; Koster, M.; Wagner, T. *Chem. Ber.* **1996**, *129*, 1099–1101. (c) Musaev, D. G.; Morokuma, K. *J. Phys. Chem.* **1996**, *100*, 6509–6517. (d) Dai, C.; Stringer, G.; Marder, T. B.; Scott, A. J.; Clegg, W.; Norman, N. C. *Inorg. Chem.* **1997**, *36*, 272–273. (e) Braunschweig, H.; Kollann, C.; Englert, U. *Eur. J. Inorg. Chem.* **1998**, 465–468. (f) Sakaki, S.; Kai, S.; Sugimoto, M. *Organometallics* **1999**, *18*, 4825–4837. (g) Sakaki, S.; Biswas, B.; Musashi, Y.; Sugimoto, M. *J. Organomet. Chem.* **2000**, *611*, 288–298. (h) Giju, K. T.; Bickelhaupt, F. M.; Frenking, G. *Inorg. Chem.* **2000**, *39*, 4776–4785. (i) Frenking, G.; Frolich, *Chem. Rev.* **2000**, *100*, 717–774. (j) Aldridge, S.; Al-Fawaz, A.; Calder, R. J.; Dickinson, A. A.; Willock, D. J.; Light, M. E.; Hursthouse, M. B. *Chem. Commun.* **2001**, 1846–1847. (k) Dickinson, A. A.; Willock, D. J.; Calder, R. J.; Aldridge, S. *Organometallics* **2002**, *21*, 1146–1157. (l) Sivignon, G.; Fleurat-Lessard, P.; Onno, J.-M.; Volatron, F. *Inorg. Chem.* **2002**, *41*, 6656–6661.

(26) Ishiyama, T.; Matsuda, N.; Murata, M.; Ozawa, F.; Suzuki, A.; Miyaura, N. *Organometallics* **1996**, *15*, 713–720.

(24) (a) Baker, R. T.; Calabrese, J. C.; Westcott, S. A.; Nguyen, P.; Marder, T. B. *J. Am. Chem. Soc.* **1993**, *115*, 4367–4368. (b) Clegg, W.; Lawlor, F. J.; Marder, T. B.; Nguyen, P.; Norman, N. C.; Orpen, A. G.; Quayle, M. J.; Rice, C. R.; Robins, E. G.; Scott, A. J.; Souza, F. E. S.; Stringer, G.; Whittell, G. R. *J. Chem. Soc., Dalton Trans.* **1998**, 301–309.

Table 2. Selected Bond Distances (Å) and Angles (deg)

	3Bpin			3Bcat		
	X-ray	neutron	calcd	X-ray	neutron	calcd
Rh–P(1)	2.3476(4)	2.347(3)	2.385	2.3395(6)	2.335(7)	2.383
Rh–P(2)	2.3442(4)	2.343(3)	2.387	2.3374(6)	2.340(7)	2.384
Rh–Cl	2.4392(4)	2.432(3)	2.483	2.4215(7)	2.415(6)	2.475
Rh–B	1.9812(15)	1.985(4)	1.971	1.965(2)	1.973(7)	1.960
Rh–H(1)	1.47(2)	1.571(5)	1.548	1.40(2)	1.531(11)	1.527
B–O(1)	1.391(2)	1.388(4)	1.395	1.422(2)	1.413(8)	1.423
B–O(2)	1.379(2)	1.392(3)	1.395	1.418(2)	1.401(7)	1.425
B···H(1)	2.02(2)	2.013(5)	2.179	2.01(2)	2.004(10)	2.021
P(1)–Rh–P(2)	163.87(1)	163.7(1)	168.9	172.65(2)	172.5(3)	173.2
P(1)–Rh–Cl	93.25(1)	93.2(1)	90.9	87.64(3)	87.4(2)	87.5
P(1)–Rh–B	94.32(4)	94.1(1)	93.5	93.36(5)	93.1(3)	95.2
P(1)–Rh–H(1)	85.6(8)	85.9(2)	87.8	87.5(8)	88.0(5)	88.4
P(2)–Rh–Cl	94.35(1)	94.3(1)	91.9	92.56(3)	92.5(2)	91.7
P(2)–Rh–B	94.70(4)	95.0(1)	95.2	91.41(5)	91.9(3)	89.9
P(2)–Rh–H(1)	84.9(8)	85.0(1)	87.7	88.8(8)	88.7(4)	89.2
Cl–Rh–B	117.73(4)	118.7(1)	113.7	137.87(5)	138.8(3)	137.6
Cl–Rh–H(1)	172.2(8)	173.5(2)	170.8	151.1(8)	152.6(4)	152.7
B–Rh–H(1)	70.0(8)	67.8(2)	75.4	70.9(8)	68.5(4)	69.6
O(2)–B–Rh–H(1)	84.3(8)	84.6(3)	63.46	17.5(9)	17.7(7)	23.9
	24.0(9) <sup>a</sup>					

<sup>a</sup> Minor position of the disordered ligand.

and potential  $\pi$ -acceptor (via the  $p\pi$  orbital on B). The distortion of the SP consists mainly of the apical boryl ligand tilting toward H(1). It is noteworthy that such a distortion does *not* lie on the transformation path between TBP and SP as envisaged by the Berry pseudorotation mechanism,<sup>27</sup> again in accordance with the theoretical predictions.<sup>22b</sup>

Alternatively, the structure could be described as a distorted trigonal bipyramid (DTBP) with the phosphine ligands in the axial positions. The equatorial plane would then be comprised of the Cl, hydride H(1), and boryl B atoms; the Rh atom lies in the same plane within experimental error. In accordance with the theoretical predictions,<sup>22</sup> the equatorial ligands would then be said to adopt the Y configuration, with the B–Rh–H angle very acute and the Cl ligand (poor  $\sigma$ -donor/good  $\pi$ -donor) opposite to this angle. However, the “Y” is rather asymmetric, Cl–Rh–B and Cl–Rh–H(1) angles differing by ca. 55°.

The X-ray study of **3Bpin** at 120 K (henceforth **3Bpin-X**) found the boryl ligand to be disordered between two orientations (A and B) with occupancies of 85.3(2) and 14.7(2)%, differing by a 66° rotation around the Rh–B bond (Figure 1b). Repeating the data collection with a different crystal sample, we observed the same mode of disorder and the same occupancies of 85.5(2) and 14.5(2)% (other parameters also agreed within experimental error; e.g., the Rh–H(1) distance of 1.44(2) and B–Rh–H(1) angle of 70.2(9)°). On the other hand, the neutron diffraction study at 20 K (**3Bpin-N**) revealed a fully ordered structure, corresponding to the major conformer A of **3Bpin-X**. Most likely, the difference is due to the different modes of cooling employed, rather than different final temperatures. In the X-ray experiment, the crystal was flash-cooled from room temperature, to avoid it deteriorating in air, thus “freezing” the disorder; in the neutron study, it was cooled very slowly, which permitted gradual relaxation into an ordered structure.

The boron atom is trigonal planar. The Rh/B/O(1)/O(2) plane and the equatorial plane of the coordination

bipyramid of Rh, i.e., the Rh/B/Cl/H(1) plane, form a dihedral angle of 81° in **3Bpin-N**. The corresponding angles in **3Bpin-X** are 82° for the major conformer (A) and 16° for the minor one (B). In each case, the five-membered BO<sub>2</sub>C<sub>2</sub> heterocycle adopts an envelope conformation. In **3Bpin-N**, the C(2) atom is displaced by 0.45 Å from the plane of the other four atoms, as it is in the A conformer of **3Bpin-X**, whereas in the B conformer, C(1) is displaced by 0.42 Å.

In other respects, the X-ray and neutron structures show no statistically significant discrepancies, as far as non-hydrogen atoms are concerned. Although the X-ray method underestimated the Rh–H bond distance by ca. 0.1 Å, which is the normal systematic error due to the shift of electron density from the H atom into the bond area, the *direction* of the bond was determined fairly accurately.

The structure of **3Bcat** (Figure 1c) shows no disorder, and there are no significant differences between the X-ray and neutron structures, except for the Rh–H(1) bond length (vide supra), or with the earlier X-ray determination at 203 K.<sup>11b</sup> As in **3Bpin**, the Rh coordination is DTBP, with the Rh, Cl, B, and H(1) atoms coplanar and with a similar narrow B–Rh–H angle. The Bcat ligand is planar within experimental error, and the Rh atom lies 0.09 Å from its mean plane. However, there are some important differences between the structures of **3Bcat** and **3Bpin**. Thus (i) while in **3Bpin**, the boryl ligand is roughly perpendicular to the equatorial plane of the Rh, in **3Bcat**, the dihedral angle between the two is only 16°, (ii) in **3Bcat**, there is much less disparity between the Cl–Rh–B and Cl–Rh–H angles, and (iii) the Rh–Cl and Rh–H(1) lengths in **3Bcat** are shorter than in **3Bpin**. The latter is probably a consequence of (ii), as in **3Bpin**, there must be significant weakening of both bonds due to mutual trans influence in the nearly linear Cl–Rh–H moiety, which is less effective in **3Bcat**, where the Cl–Rh–H angle is ca. 20° smaller.

Only two Rh complexes containing hydride ligands (in both cases terminal) have been previously characterized by neutron diffraction, viz. ( $\eta$ -C<sub>5</sub>Me<sub>5</sub>)Rh(SiEt<sub>3</sub>)<sub>2</sub>(H)<sub>2</sub>

(at 20 K)<sup>28</sup> and (Ph<sub>3</sub>P)<sub>4</sub>RhH·<sup>1/2</sup>C<sub>6</sub>H<sub>6</sub> (at 250 K).<sup>29</sup> Both are rather dissimilar from **3Bpin** and **3Bcat**, being formally Rh<sup>V</sup> and Rh<sup>I</sup>, respectively. The Rh–H bonds in the former average 1.581(3) Å (close to our results), and the latter structure is of rather low precision (*R* = 12.6%), so that the Rh–H distance of 1.31 Å is not reliable. In the 11 fully determined X-ray structures of 5-coordinate, 16-electron Rh<sup>III</sup> hydride complexes available in the Cambridge Structural Database<sup>30</sup> (Nov 2002 update), the Rh–H distances vary from 1.12 to 1.77(13) Å—an indication of the large random, as well as systematic, experimental errors. However, most of these structures were determined at room temperature.<sup>31</sup> The few low-temperature studies give more consistent values of 1.45(3) Å in triclinic (P<sup>i</sup>Pr<sub>3</sub>)<sub>2</sub>Rh(H)<sub>2</sub>Cl at 173 K,<sup>32</sup> 1.48(3) Å in its monoclinic polymorph at 220 K,<sup>33</sup> and 1.46(2) Å in (P<sup>i</sup>Pr<sub>3</sub>)<sub>2</sub>RhH(OSO<sub>2</sub>CF<sub>3</sub>)(COMe) at 120 K,<sup>34</sup> all of which are close to our X-ray results. As the X-ray technique is generally more reliable in determining the direction, rather than the length, of the metal–hydride bond (vide supra), it is noteworthy that all these complexes display coordination polyhedra similar to those of **3Bpin** and **3Bcat** and to those of the theoretical model, which can be described as Y-type DTBP or a severely distorted SP. Invariably, two phosphine ligands occupy trans positions (axial in TBP), and a relatively weak  $\sigma$ -donor ligand (Cl, I, F<sub>3</sub>CSO<sub>3</sub>, Ph<sub>3</sub>BCN) lies opposite the narrow angle of the equatorial “Y” configuration; the latter angle is formed between a hydride and a silyl, acyl, alkyl, or another hydride ligand and varies from 64 to 89° (65 to 72° for H–Rh–H). In the two cases, when a “single-faced”  $\pi$ -acceptor ligand (acetyl<sup>34a</sup> or benzoyl<sup>34b</sup>) was present, it was coplanar with the equatorial plane of the TBP (similar to **3Bcat** but not to **3Bpin**). Although the electronically preferable orientations of such ligands were analyzed extensively for TBP complexes of d<sup>8</sup>–d<sup>10</sup> metals,<sup>35</sup> for d<sup>6</sup> metals this question has not been well studied. As discussed above, the structurally characterized complexes (PR<sub>3</sub>)<sub>2</sub>RhCl(boryl)<sub>2</sub><sup>24</sup> have Rh coordination intermediate between SP and DTBP. In the DTBP description, the phosphine ligands are axial and the Cl ligand lies opposite the narrow B–Rh–B angle (78–79°) of the Y-shaped equatorial configuration. One Bcat ligand is coplanar with the equatorial plane and the other is perpendicular to it. The latter forms substantially shorter Rh–B bonds than the former: 1.956(8) vs 2.008(7) Å in (PPh<sub>3</sub>)<sub>2</sub>RhCl(Bcat)<sub>2</sub>·3C<sub>2</sub>H<sub>4</sub>Cl<sub>2</sub>,<sup>24a</sup> 1.954(4) vs 2.008(4) Å in (PPh<sub>3</sub>)<sub>2</sub>RhCl(Bcat)<sub>2</sub>·4CH<sub>2</sub>Cl<sub>2</sub>,<sup>24b</sup> 1.973(2) vs 1.994(2) Å in (PEt<sub>3</sub>)<sub>2</sub>RhCl(Bcat)<sub>2</sub>,<sup>24b</sup> 1.91(1) vs 2.03(1) Å in (PPh<sub>3</sub>)<sub>2</sub>RhCl(Bcat-

Me)<sub>2</sub>·3CH<sub>2</sub>Cl<sub>2</sub>·<sup>1/2</sup>C<sub>6</sub>H<sub>14</sub>.<sup>24b</sup> Thus, these structural comparisons suggest that the perpendicular conformation is more favorable for interactions with the Rh d orbitals, although the extent of metal (d)–boryl (p)  $\pi$ -interactions is still subject to debate. On the other hand, the X-ray structure of (P<sup>i</sup>Pr<sub>3</sub>)<sub>2</sub>IrH(Cl)(Ph)<sup>23a</sup> and the calculations of its model (PH<sub>3</sub>)<sub>2</sub>IrH(Cl)(Ph)<sup>22a</sup> show the equatorial orientation of the phenyl ring and a narrow C–Rh–H angle (78° experimental, 80° calculated), with no evidence of even a weak bonding interaction between the ipso-C atom of the phenyl and the hydride ligand.<sup>22a</sup>

B–O bonds in **3** are substantially shorter than the sum of single-bond covalent radii of B (0.82 Å) and O (0.70 Å),<sup>36</sup> indicating  $\pi$  bonding between the lone electron pairs of O and the empty p $\pi$  orbital of B. However, this bonding is weakened by competition with the d(Rh)  $\rightarrow$  p(B) back-donation, as is evident on comparison of **3** with corresponding diboranes, where the B<sub>2</sub>O<sub>4</sub> moiety is a six-atom eight- $\pi$ -electron system; hence, the central B–B bond has no  $\pi$ -component (indeed, its length of 1.68–1.72 Å is twice the covalent radius of B) and offers no competition to the B–O  $\pi$ -bonding. Thus, the B–O distances in **3Bpin** are longer than in B<sub>2</sub>pin<sub>2</sub> (1.324 Å),<sup>37</sup> di- and tetraphenyl derivatives of bis(ethane-1,2-diolato)diborane (1.368(3) and 1.360(2) Å, respectively),<sup>38</sup> and (MeO)<sub>2</sub>B–B(OMe)<sub>2</sub> (1.368(3) Å from gas electron diffraction).<sup>39</sup> Likewise, the B–O distances in **3Bcat** are longer than in B<sub>2</sub>cat<sub>2</sub> (1.388(2) Å) and its di- and tetra-*tert*-butyl derivatives (1.386(3) and 1.384(3) Å, respectively).<sup>40</sup> Similar B–O distances of 1.381(2) Å were observed<sup>41</sup> in isomorphous crystals of Cl–Bcat and Br–Bcat, where no  $\pi$ -electron transfer from the halogen to the boron atom was observed. Note also that the B–O bonds in Bcat moieties, both in diboranes and in **3**, are proportionally longer than in the saturated Bpin analogues. This results from the fact that the benzene ring also competes for the  $\pi$ -electron pairs of O and from the difference in C–O–B bond angles in the two ring systems. In the Bcat moiety, the ring strain is expected to be greater than in Bpin. Rh<sup>I</sup> being a much better back-donor than Rh<sup>III</sup>, it is interesting that B–O bonds in the trigonal-bipyramidal complex (Me<sub>3</sub>P)<sub>4</sub>Rh–Bcat<sup>25d</sup> are slightly weaker (1.429(3) Å) than in **3Bcat**.

**Theoretical Study of the Structure and Bonding in (PR<sub>3</sub>)<sub>2</sub>RhHCl(Boryl) Complexes.** As mentioned above, the main structural differences observed between the complexes **3Bcat** and **3Bpin** are the orientation of the BO<sub>2</sub> plane and the Cl–Rh–B angle. The Bcat complex adopts a roughly coplanar orientation of the BO<sub>2</sub> plane with respect to the RhHCIB plane and has a

(28) Fernandez, M. J.; Bailey, P. M.; Bentz, P. O.; Ricci, J. S.; Koetzle, T. F.; Maitlis, P. M. *J. Am. Chem. Soc.* **1984**, *106*, 5458–5463.

(29) Mclean, M. R.; Stevens, R. C.; Bau, R.; Koetzle, T. F. *Inorg. Chim. Acta* **1989**, *166*, 173.

(30) Allen, F. H. *Acta Crystallogr., Sect. B* **2002**, *58*, 380–388.

(31) (a) Crocker, C.; Errington, R. J.; McDonald, W. S.; Odell, K. J.; Shaw, B. L.; Goodfellow, R. J. *J. Chem. Soc., Chem. Commun.* **1979**, 498–499. (b) Osakada, K.; Koizumi, T.; Yamamoto, T. *Organometallics* **1997**, *16*, 2063–2069. (c) Carlton, L.; Weber, R.; Levendis, D. C. *Inorg. Chem.* **1998**, *37*, 1264–1271. (d) Nishihara, Y.; Takemura, M.; Osakada, K. *Organometallics* **2002**, *21*, 825–831.

(32) Harlow, R. L.; Thorn, D. L.; Baker, R. T.; Jones, N. L. *Inorg. Chem.* **1992**, *31*, 993–997.

(33) Butler, D. C. D.; Bruce, D. W.; Lightfoot, P.; Cole-Hamilton, D. J. *Can. J. Chem.* **2001**, *79*, 472–478.

(34) (a) Goikhan, R.; Milstein, D. *Angew. Chem., Int. Ed.* **2001**, *40*, 1119–1122. (b) Wang, K.; Emge, T. J.; Goldman, A. S.; Li, C.; Nolan, S. P. *Organometallics* **1995**, *14*, 4929–4936.

(35) Rossi, A. R.; Hoffmann, R. *Inorg. Chem.* **1975**, *14*, 365–374.

(36) Sanderson, R. *J. Am. Chem. Soc.* **1983**, *105*, 2259–2261.

(37) Nöth, H. Z. *Naturforsch.* **1984**, *39b*, 1463–1466.

(38) Clegg, W.; Johann, T. R. F.; Marder, T. B.; Norman, N. C.; Orpen, A. G.; Peakman, T. M.; Quayle, M. J.; Rice, C. R.; Scott, A. J. *J. Chem. Soc., Dalton Trans.* **1998**, 1431–1438. Clegg, W.; Lawlor, F. J.; Lesley, G.; Marder, T. B.; Norman, N. C.; Orpen, A. G.; Quayle, M. J.; Rice, C. R.; Scott, A. J. *J. Organomet. Chem.* **1998**, 183–192.

(39) Brain, P. T.; Downs, A. J.; Maccallum, P.; Rankin, D. W. H.; Robertson, H. E.; Forsyth, G. A. *J. Chem. Soc., Dalton Trans.* **1991**, 1195–1200.

(40) Nguyen, P.; Lesley, G.; Taylor, N. J.; Marder, T. B.; Pickett, N. L.; Clegg, W.; Elsegood, M. R. *J. Inorg. Chem.* **1994**, *33*, 4623–4624. Clegg, W.; Elsegood, M. R. J.; Lawlor, F. J.; Norman, N. C.; Pickett, N. L.; Robins, E. G.; Scott, A. J.; Nguyen, P. *Inorg. Chem.* **1998**, *37*, 5289–5293.

(41) Coapes, R. B.; Souza, F. E. S.; Fox, M. A.; Batsanov, A. S.; Goeta, A. E.; Yufit, D. S.; Leech, M. A.; Howard, J. A. K.; Scott, A. J.; Clegg, W.; Marder, T. B. *J. Chem. Soc., Dalton Trans.* **2001**, 1201–1209.

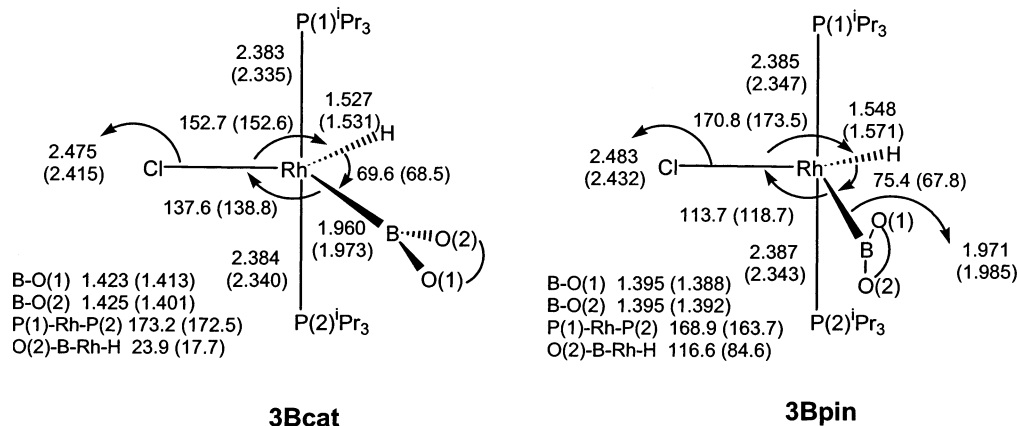


**Figure 2.** Comparison of selected calculated and experimental structural parameters (bond lengths in Å and bond angles in deg) for **3Bcat** and **3Bpin**. The parameters shown in parentheses are from the neutron diffraction data.

relatively large Cl–Rh–B angle, while the Bpin complex prefers a perpendicular BO<sub>2</sub> orientation and gives a small Cl–Rh–B angle. To understand these differences and the bonding in these compounds in general, calculations have been carried out on a series of (PR<sub>3</sub>)<sub>2</sub>RhHCl(boryl) complexes. The phosphine ligands used were PH<sub>3</sub> (**1**), PMe<sub>3</sub> (**2**), and P<sup>i</sup>Pr<sub>3</sub> (**3**), and the boryl ligands employed were Bcat and Bpin.

Initially, geometries of complexes **1–3** were optimized to understand the structural differences. These calculations show that both **1Bcat** and **1Bpin** favor perpendicular conformations. The same is true for PMe<sub>3</sub> complexes, **2Bcat** and **2Bpin**. However, introduction of bulkier P<sup>i</sup>Pr<sub>3</sub> ligands results in different conformations for **3Bcat** (coplanar) and **3Bpin** (perpendicular). The optimized and experimental geometries for **3Bcat** and **3Bpin** are shown in Figure 2. The calculated bond distances and angles, including Cl–Rh–B, reproduce the experimental results quite well.

On the basis of the results of the above calculations, we conclude that there is a strong structural preference for a perpendicular orientation of the boryl ligands in the complexes studied here and that only the P<sup>i</sup>Pr<sub>3</sub> systems can reproduce the experimental observations. To investigate further the reasons behind the conclusions summarized above, we calculated both perpendicular (defined as **A**) and coplanar (defined as **B**) structural forms for all of the complexes. For a given (PR<sub>3</sub>)<sub>2</sub>RhHCl(boryl) complex, it is found that only structural form A or B corresponds to a minimum on the potential energy surface. To this end, we partially optimized either the perpendicular (**A**) or coplanar (**B**) form, if it did not correspond to a minimum, through the constraint of the O–B–Rh–H (hydride) dihedral angle. For **3Bcat** and **3Bpin**, conformational isomers with different orientations of the isopropyl groups are possible. The conformations observed in the X-ray crystal structures of complexes **3Bcat** and **3Bpin** were considered. To obtain the structural forms of **3BcatA** and **3BpinB**, the observed conformation of the isopropyl groups in **3Bpin** was used, as the calculated energies of these conformations are relatively lower than others.

Figures 3 and 4 show the calculated structures (together with the relative energies of the perpendicular (**A**) and coplanar (**B**) structural forms) for the Bcat and Bpin complexes, respectively. Energetically, although the coplanar structures are generally less stable than

their perpendicular counterparts, they become relatively more and more stable for both Bcat and Bpin complexes with the change in the phosphine ligands from PH<sub>3</sub> to PMe<sub>3</sub> and then to P<sup>i</sup>Pr<sub>3</sub>. For the Bcat complexes, **3BcatB** (the coplanar structural form) is found to be more stable than **3BcatA** (the perpendicular form). For the Bpin complexes, the coplanar structural form **3BpinB** is still higher in energy than the perpendicular form **3BpinA**, although the energy difference between the two forms became smaller. These results are consistent with the experimental findings that a roughly perpendicular structural form is observed for **3Bpin** while a coplanar structural form is adopted for **3Bcat**. One might question the validity of our claim regarding the stability of **3Bcat** on the basis of the small energy difference of 0.8 kcal/mol. However, the stability trends observed for both the Bcat and Bpin complexes suggest that the calculated relative energies are reliable.

Geometrically, we find that, for complexes **1Bcat** and **1Bpin** with PH<sub>3</sub> as the phosphine ligands, the three equatorial ligands together with the metal center are arranged in an asymmetric Y-shaped structure for both the perpendicular and coplanar structural forms. When PMe<sub>3</sub> or P<sup>i</sup>Pr<sub>3</sub> is used as the phosphine ligand, the Cl–Rh–B angles decrease drastically when compared to the PH<sub>3</sub> cases, except for the coplanar structural forms of Bcat complexes (see **2BcatB** and **3BcatB** in Figure 3), in which the Cl–Rh–B angles change only slightly.

**Stability of the Perpendicular Structural Forms.** Clearly, all of the calculated structures shown in Figures 3 and 4 adopt either a Y-shaped structure or one which is intermediate between Y-DTBP and a distorted-SP structure. The B–Rh–H angles in all the structures are calculated to be less than 80.0°, implying hydride–boryl interactions. From Figures 3 and 4, one can also see that there is a strong preference for a perpendicular structural form for these boryl complexes. It is expected that the hydride–boryl interactions are favorable in the perpendicular structural form. The Wiberg bond indices listed in Table 3 from the NBO analysis show that the B···H interactions for all structures are significant and that the perpendicular structures have in general a stronger B···H interaction than their coplanar forms. In addition to the favorable B···H interactions, one cannot overlook the fact that the “empty” pπ orbital of the boryl ligand favors the filled dπ orbitals in the equatorial plane for π-back-donation.<sup>35</sup>

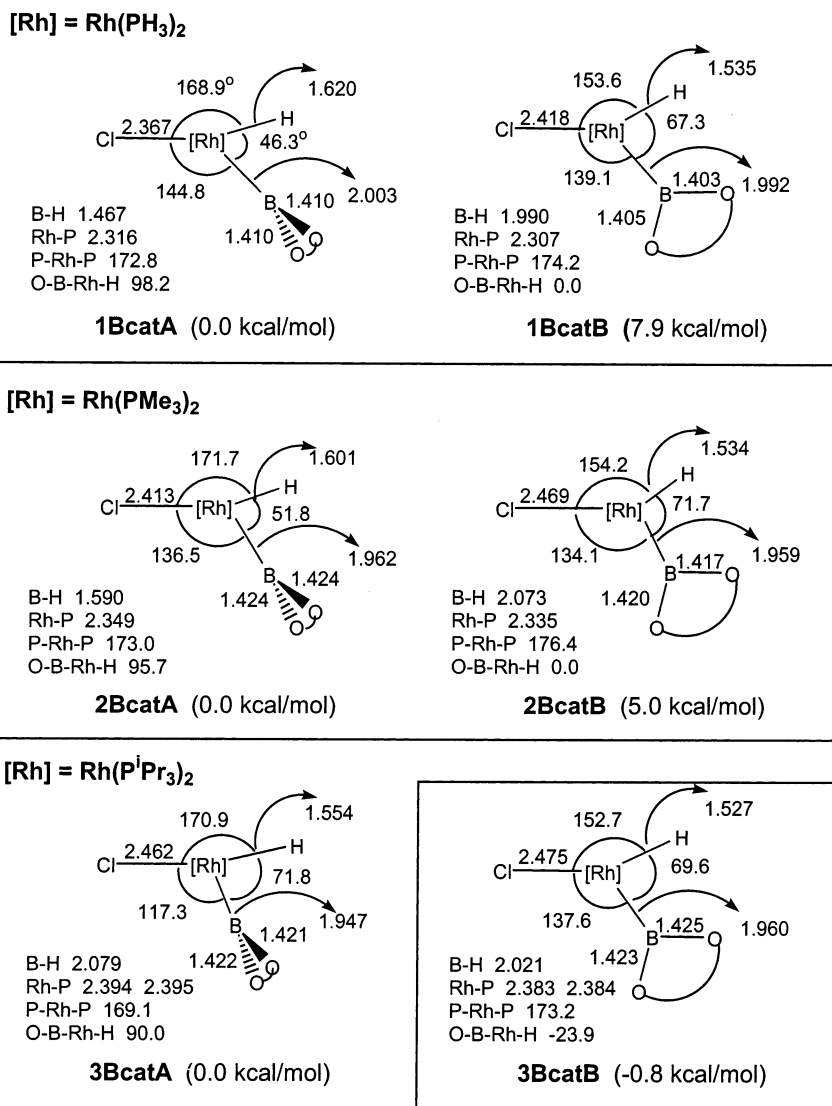


**Figure 3.** Calculated bond lengths (Å) and bond angles (deg) of the (PR<sub>3</sub>)<sub>2</sub>RhClBcat complexes with the perpendicular and coplanar structural forms, together with their relative energies. The two phosphine ligands are roughly perpendicular to the molecular plane shown in the figure and are omitted for the purpose of clarity. Structure **3BcatB** is the optimized structure for PR<sub>3</sub> = P<sup>i</sup>Pr<sub>3</sub> and also corresponds to the experimental structure.

With the increase of electron donation ability of the phosphine ligands in **1** to **3**, the metal-to-boryl  $\pi$ -back-donation increases because of the increasing electron richness at the metal center. As a result, the H–Rh–B angles increase, leading to a decrease in the Cl–Rh–B angles. The increase in back-donation interactions is evidenced by a shortening of the Rh–B bonds along the series **1**–**3**. The increase in the H–Rh–B angles along the series weakens the B···H interactions, giving stronger Rh–H bonds.

**Geometrical Changes in the Coplanar Structural Forms with Different Phosphine Ligands.** When the phosphine ligands change from PH<sub>3</sub> to PMe<sub>3</sub> and then to P<sup>i</sup>Pr<sub>3</sub>, the perpendicular structural forms (**A**) experience a drastic decrease in the Cl–Rh–B bond angle. The structures change from a Y shape to one closer to the SP structure (T shape) for both the Bcat and Bpin complexes. However, for the coplanar structural forms (**B**), similar changes are observed only for the Bpin complexes, while the Cl–Rh–B angles remain roughly unchanged for the Bcat complexes.

As mentioned earlier, the SP configuration would be preferred in the presence of a strong  $\sigma$ -donor ligand. To adopt a Y-shaped structure, such as **1BcatA** and **1BpinA**, significant stabilization from other interactions is needed. We expect that the B···H interactions are very significant for **1BcatA** and **1BpinA**. With increasing electron richness at the metal center as more basic phosphines are employed, the boron gains electron density directly from the metal center, weakening the B···H interactions and leading to structures closer to the SP T shape. In other words, for the perpendicular structural forms of PMe<sub>3</sub> and P<sup>i</sup>Pr<sub>3</sub> complexes, the B···H interactions are not strong enough to yield a Y-shaped structure. This is as expected, because stronger donor phosphine ligands favor oxidative addition of B–H leading to weaker residual B–H interactions, whereas weaker donor ligands lead to  $\sigma$ -H–B(OR)<sub>2</sub> complexes. Thus, with PH<sub>3</sub>, **1BcatA** and **1BpinA** are calculated to be stretched  $\sigma$ -borane complexes with geometries fairly close to those in Ziegler's model compounds<sup>10c</sup> (Table 1).



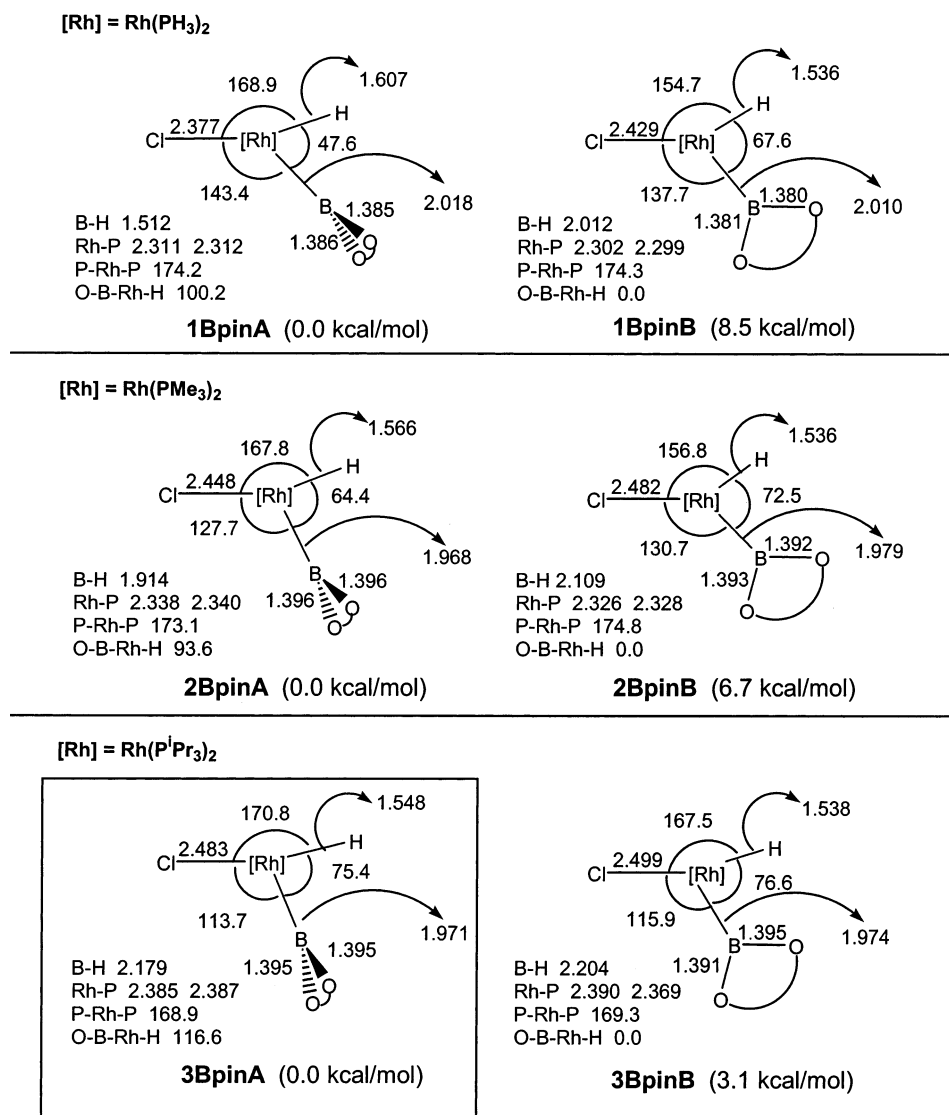


**Figure 4.** Calculated bond lengths (Å) and bond angles (deg) of the (PR<sub>3</sub>)<sub>2</sub>RhHClBpin complexes with the perpendicular and coplanar structural forms, together with their relative energies. The two phosphine ligands are roughly perpendicular to the molecular plane shown in the figure and are omitted for the purpose of clarity. Structure **3BpinA** is the optimized structure (PR<sub>3</sub> = P<sup>i</sup>Pr<sub>3</sub>) and also corresponds to the experimental structure.

**Table 3. Wiberg Bond Indices for the Bcat and Bpin Complexes**

	Rh–B	B···H		Rh–B	B···H
<b>1BcatA</b>	0.591	0.486	<b>1BpinA</b>	0.574	0.450
<b>1BcatB</b>	0.691	0.199	<b>1BpinB</b>	0.665	0.192
<b>2BcatA</b>	0.692	0.412	<b>2BpinA</b>	0.731	0.254
<b>2BcatB</b>	0.757	0.179	<b>2BpinB</b>	0.733	0.170
<b>3BcatA</b>	0.795	0.202	<b>3BpinA</b>	0.770	0.167
<b>3BcatB</b>	0.749	0.200	<b>3BpinB</b>	0.766	0.145

From Figures 3 and 4, the decrease in Cl–Rh–B angle from **1** to **3** in the perpendicular form is more dramatic than it is in the coplanar form. This implies that there is less tendency to adopt SP configurations in the coplanar forms compared to the perpendicular forms. Therefore, it is expected that only moderate B···H interactions should be enough to keep the coplanar forms in a Y-shaped structure. The calculated structures for the coplanar forms suggest that the B···H interactions for the Bcat complexes are stronger than those for the Bpin complexes. Therefore, with the increase in electron richness at the metal center (**1** < **2** < **3**), the Bpin complexes adopt the distorted-SP structures while

the Bcat complexes retain the DTBP structure (see the coplanar structural forms of Figures 3 and 4).

**Different Electronic Behaviors of the Bcat and Bpin Ligands.** As mentioned above, significant B···H interactions are found for both the perpendicular and coplanar structural forms in the boryl complexes on the basis of the calculated structural parameters as well as the NBO Wiberg bond index analyses (Table 3). It is easily understood that there is a strong B···H interaction for a perpendicular structural form, because the “empty” p orbital of the boryl ligand can effectively overlap with the metal–hydride bonding orbital. To account for the B···H interaction in a coplanar structural form, one has to invoke the  $\sigma^*$  antibonding orbital derived from boron and the two substituents of the boryl ligand. In other words, both the “empty” p orbital, which is  $\pi^*$  antibonding with respect to the substituents, and the BO<sub>2</sub>  $\sigma^*$ -orbital are important in the back-bonding interactions. Figure 5 schematically illustrates these two empty orbitals, which act as electron acceptors. It should be noted that extensive mixings among orbitals



**Figure 5.** Schematic illustration of the  $\pi^*$  and  $\sigma^*$  orbitals in the  $BX_2$  ligand.

of the  $\pi^*$  type (as well as among those of  $\sigma^*$  type) occur in the frontier orbitals of the Bcat or Bpin groups. It is difficult to single out representative  $\sigma^*$  and  $\pi^*$  orbitals corresponding to the two schematic orbitals shown in Figure 5, which are provided for the purpose of conceptual illustration.

Because of the geometrical requirement, the B–O  $\sigma$  interactions are relatively weaker in the Bcat ligand when compared to those in the Bpin ligand. The B–O bond distances differ by 0.02 Å between the two ligands. We expect that the electron-accepting ability of the Bcat ligand's B–O  $\sigma^*$  orbital is greater than that of the Bpin ligand's  $\sigma^*$  orbital (see Figure 5). Population analyses of HBcat and HBpin indeed show that the p orbital used for  $\sigma^*$  (labeled  $p(\sigma^*)$ ) has higher population (0.385) for HBpin than that (0.364) for HBcat, indicating its poorer acceptor ability. The p orbital used for  $\pi^*$  (labeled as  $p(\pi^*)$ ) has a similar population (0.365) for HBpin and for HBcat (0.369). In other words, the electron-accepting abilities of  $\sigma^*$  and  $\pi^*$  of Bcat are expected to be closer to one another when compared with those of Bpin.

**Trends in the Relative Stabilities of the Coplanar and Perpendicular Structures.** While the perpendicular structural forms are generally preferred in these boryl complexes, we notice that the energy difference between the two structural forms for each Bcat complex is smaller than that for its corresponding Bpin complex. The stability order is switched for the two boryl complexes **3Bcat** and **3Bpin**, containing  $P^iPr_3$  ligands. Clearly, the energetic difference should be related to the different electronic behaviors of the Bcat and Bpin ligands. As discussed above, the  $\sigma^*$  and  $\pi^*$  orbitals which are perpendicular to each other and responsible for back-bonding interactions with metal fragments (including metal  $d\pi$  electrons and metal–hydride bonding electrons) differ less significantly in terms of their back-bonding interaction abilities for the Bcat ligand than those for the Bpin ligand. It is therefore anticipated that the energy difference between the perpendicular and coplanar structural forms for a Bcat complex is smaller when compared to that for an analogous Bpin complex.

With increasing electron donation ability of the phosphine, the coplanar structural forms gain more stability as the calculation results show. Along the series **1**, **2**, and **3**, the relative energies of **A** and **B** structural forms for both the Bcat and Bpin systems decrease. As there is no apparent electronic reason for increased stability of the coplanar structural forms along the series, we believe that steric effects play an important role here. Clearly, steric factors favor the coplanar structures. Along the series **1**, **2**, and **3**, steric effects increase in importance. Therefore, the energy differences decrease when the steric repulsion becomes greater. Because of

the intrinsically smaller energy difference between the perpendicular and coplanar structural forms for a Bcat complex as discussed above, the coplanar structural form becomes preferred for **3Bcat**, in which very bulky phosphine ligands are present. For **3Bpin**, the steric factor does not overcome the intrinsic higher energy difference. Therefore, the **3Bpin** complex still adopts the commonly preferred perpendicular structural form.

## Conclusions

Single crystal X-ray and especially neutron diffraction studies, the latter at 20 K, on  $(P^iPr_3)_2RhHCl(Bcat)$  (**3Bcat**) and  $(P^iPr_3)_2RhHCl(Bpin)$  (**3Bpin**) complexes provide the first accurate location of hydrogens in a metal boryl hydride complex. While the fundamental structures of the two complexes are quite different with regard to the orientation of the boryl ligand and the Cl–Rh–B angles, the H–Rh–B angles of ca. 68° lead to B··H separations of ca. 2.0 Å, indicating that a  $Rh^{III}$  boryl hydride formulation is appropriate, with residual B··H interaction in both cases.

Density functional theory calculations have been performed to study structural preferences and bonding in  $(PR_3)_2RhHCl(Bcat)$  and  $(PR_3)_2RhHCl(Bpin)$  complexes with different phosphine ligands. Factors influencing the different orientations of the boryl ligands as well as the Cl–Rh–B angles observed in the experimental structures of **3Bpin** and **3Bcat** have been analyzed. In general, boryl ligands in such systems prefer a perpendicular orientation with respect to the equatorial plane of the distorted-trigonal-bipyramidal structure adopted by these boryl complexes. The theoretical study confirms the residual B··H interaction in both **3Bpin** and **3Bcat**, indicating that a B–H interaction can occur through both the “empty”  $BO_2$   $p(\pi^*)$  and  $BO_2$   $\sigma^*$  orbitals, which are mutually perpendicular. The latter interaction has not been addressed in previous studies. Our detailed analyses reveal that interactions between Rh–H and these two perpendicular orbitals of the Bcat ligand differ less significantly than with those of the Bpin ligand. This intrinsic bonding feature makes the energy difference between the perpendicular and coplanar structures smaller for a given Bcat complex than for its Bpin analogue, allowing the observed coplanar form for **3Bcat** when steric effects of  $P^iPr_3$  become significant.

For a 16-electron  $ML_5$  complex, both square-pyramidal (T-shaped) and distorted-trigonal-bipyramidal (Y-shaped) structures are possible. Calculations show that, for the boryl complexes studied in this paper, a perpendicular form has a strong tendency to adopt structures ranging from a T shape to an intermediate between T- and Y-shaped structures. Increasing the electron-donating properties of the phosphine ligands yields a structure closer to the T-shaped end, in which the Cl–Rh–B angle is smaller, with **3BpinA** providing an example. Calculations also show that a coplanar form favors structures ranging from a Y shape to an intermediate between the T- and Y-shaped structures. The moderately strong B··H interaction through the hydride and the empty B–O<sub>2</sub>  $\sigma^*$  orbital of the Bcat ligand leads to the larger Cl–Rh–B angle observed for the coplanar structure of **3Bcat**.

It is clear from the experimental and theoretical study that relatively small changes in either electronic or

Table 4. Crystal Data and Experimental Details

	3Bpin		3Bcat	
formula	C <sub>24</sub> H <sub>55</sub> BClO <sub>2</sub> P <sub>2</sub> Rh		C <sub>24</sub> H <sub>47</sub> BClO <sub>2</sub> P <sub>2</sub> Rh	
mol mass (amu)	586.79		578.73	
cryst syst	monoclinic		monoclinic	
space group, Z	P2 <sub>1</sub> /n (No. 14), 4		P2 <sub>1</sub> /c (No. 14), 4	
CCDC dep no.	151582	206109	206110	206111
radiation	Mo K $\alpha$	neutron	Mo K $\alpha$	neutron
$\lambda$ , Å	0.710 73	1.5478(5)	0.710 73	1.5453(5)
T (K)	120	20	120	20
a (Å)	10.691(1)	10.637(1)	11.228(3)	11.181(3)
b (Å)	14.990(1)	14.903(1)	11.101(3)	11.050(3)
c (Å)	19.129(1)	19.183(1)	23.414(7)	23.233(7)
$\beta$ (deg)	91.12(1)	90.688(4)	102.28(4)	102.32(2)
V (Å <sup>3</sup> )	3065.0(4)	3040.5(4)	2851.6(14)	2804.3(14)
cryst size (mm)	0.65 × 0.55 × 0.12	1.8 × 2.0 × 4.0	0.6 × 0.4 × 0.2	1.3 × 2.5 × 3.5
$\mu$ (mm <sup>-1</sup> )	0.77	0.37	0.60	0.35
total no. of rflns	40 809	11 319	33 082	5358
no. of unique rflns	8120	3687	7624	2356
abs cor	integration	integration	multiscan	integration
transmission	0.677–0.913	0.314–0.603	0.627–0.819	0.331–0.643
R <sub>int</sub>	0.064, <sup>a</sup> 0.027	0.051	0.059, <sup>a</sup> 0.029	0.057
no. of rflns, I > 2 $\sigma$ (I)	7531	3355	7021	1908
no. of variables	359	776	354	473
R(F <sup>2</sup> > 2 $\sigma$ (F <sup>2</sup> ))	0.022	0.044	0.026	0.065
R <sub>w</sub> (F <sup>2</sup> ) (all data)	0.052	0.105	0.057	0.166

<sup>a</sup> Before absorption correction.

steric factors can influence quite dramatically the structures of these compounds. Due care must be taken in the interpretation of calculations of optimized structures and reaction mechanisms using model complexes, and efforts should be made, where computing resources are available, to examine real ligands whenever possible.

### Experimental Section

Compounds **3Bpin** and **3Bcat** were synthesized according to the published routes, and details of the characterization were as reported in the earlier work.<sup>7,11b</sup>

**Crystallography.** X-ray diffraction experiments were carried out on a SMART three-circle diffractometer with a 1K CCD area detector, using graphite-monochromated Mo K $\alpha$  radiation ( $\lambda = 0.710 73$  Å) and a Cryostream (Oxford Cryosystems) open-flow N<sub>2</sub> gas cryostat. A full sphere of reciprocal space ( $2\theta \leq 58^\circ$ ) was covered by a combination of five sets of  $\omega$  scans, each set being at different  $\varphi$  and/or  $2\theta$  angles. Reflection intensities were integrated using the SAINT program<sup>42</sup> and corrected for absorption by numerical integration<sup>43</sup> based on crystal face indexing (for **3Bpin**) or by semiempirical methods based on the intensities of Laue equivalents, using SADABS software<sup>44</sup> (for **3Bcat**). The structures were solved by direct methods and refined by full-matrix least squares against  $F^2$  values of all data, using SHELXTL software.<sup>43</sup>

Neutron diffraction experiments were carried out on the four-circle thermal neutron diffractometer D19 at the ILL. The crystals were cooled using a two-stage Displex cryorefrigerator.<sup>45</sup> For **3Bpin**, 3101 reflections with low  $2\theta$  values were measured using the usual D19  $4^\circ \times 64^\circ$  curved multiwire position-sensitive gas detector,<sup>46</sup> while 8496 high-angle reflec-

tions were measured with a new flat  $64 \times 64$  2-D multiwire position-sensitive detector (wire spacing 3 mm, sample-detector distance 55 cm, area  $19^\circ \times 19^\circ$ ).<sup>47</sup> Intensity measurements were made using the two detectors simultaneously. For **3Bcat**, 1696 low-angle reflections were measured with the "banana" detector and 3834 high-angle reflections with the flat high-angle detector. Reflection intensities were integrated using the Retreat program<sup>48</sup> and corrected for neutron attenuation by Gaussian integration using the program D19abs based on the Cambridge Crystallography Subroutine Library.<sup>49</sup> The two sets of data were scaled on the basis of common reflections and merged. With the coordinates from the X-ray structure determinations as a starting point, the structures were refined against  $F^2$  for all data, using SHELXTL software<sup>43</sup> and neutron scattering amplitudes from Sears.<sup>50</sup>

Crystal data and experimental details are summarized in Table 4, and full structural information has been deposited with the Cambridge Crystallographic Data Centre as Supplementary Publication Nos. CCDC-151582 and 206109-206111.

**Computations.** Geometry optimizations for all complexes were performed at the Becke3PW91<sup>51</sup> (B3PW91) level. The effective core potentials (ECPs) of Hay and Wadt with a double- $\xi$  valence basis set (LanL2DZ)<sup>52</sup> were used to describe the Rh, Cl, and P atoms with the polarization functions for P ( $\xi_d(P) = 0.340$ ), Cl ( $\xi_d(Cl) = 0.340$ ), and Rh ( $\xi_r(Rh) = 1.235$ ).<sup>53</sup> For the model complexes **1Bcat** and **1Bpin**, the 6-31G basis set<sup>54</sup> was used for all other atoms. Polarization functions have been added for the B and H atoms ( $\xi_d(B) = 0.8$  and  $\xi_p(H) = 1.0$ ) which are directly coordinated to the metal center. The

(47) Buffet, J. C.; Guerard, B.; Viande, G. Personal communication, 2001.

(48) Wilkinson, C.; Khamis, H. W.; Stansfield, R. F. D.; McIntyre, G. J. *J. Appl. Crystallogr.* **1985**, *21*, 471–478.

(49) Matthewman, J. C.; Thompson, P.; Brown, P. J. *J. Appl. Crystallogr.* **1982**, *15*, 167–173.

(50) Sears, V. F. *Neutron News* **1992**, *3*(3), 26–27.

(51) (a) Burke, K.; Perdew, J. P.; Wang, Y. In *Electronic Density Functional Theory, Recent Progress and New Directions*, Dobson, J. F., Vinnale, G., Das, M. P., Eds.; Plenum: New York, 1998. (b) Perdew, J. P.; Burke, K.; Wang, Y. *Phys. Rev. B* **1996**, *54*, 16533–16539.

(52) (a) Hay, P. J.; Wadt, W. R. *J. Chem. Phys.* **1985**, *82*, 270–283. (b) Wadt, W. R.; Hay, P. J. *J. Chem. Phys.* **1985**, *82*, 284–298. (c) Hay, P. J.; Wadt, W. R. *J. Chem. Phys.* **1985**, *82*, 299–310.

(53) Ehlers, A. W.; Bohme, M.; Dapprich, S.; Gobbi, A.; Hollwarth, A.; Jonas, V.; Kohler, K. F.; Stegmann, R.; Veldkamp, A.; Frenking, G. *Chem. Phys. Lett.* **1993**, *208*, 111–114.

(42) SMART, Version 5.054, and SAINT, Version 6.01; Bruker AXS, Madison, WI, 1999.

(43) SHELXTL, Version 5.10; Bruker AXS, Madison, WI, 1998.

(44) Sheldrick, G. M. SADABS; University of Göttingen, Göttingen, Germany, 1998.

(45) Archer, J.; Lehmann, M. S. *J. Appl. Crystallogr.* **1986**, *19*, 456–458.

(46) Thomas, M.; Stansfield, R. F. D.; Berneron, M.; Filhol, A.; Greenwood, G.; Jacobs, J.; Felton, D.; Mason, S. A. In *Position-Sensitive Detection of Thermal Neutrons*; Convert, P., Forsyth, J. B., Eds.; Academic Press: London, 1983; p 344.

same basis sets were applied for the model complexes **2Bcat**, **3Bcat**, **2Bpin**, and **3Bpin**, except for the methyl groups and isopropyl groups on the phosphine ligands, where the STO-3G basis set<sup>55</sup> was used, considering the limited computational resources and the size of the systems studied. Single-point energy calculations based on these optimized geometries were made with a larger basis set to evaluate the relative energies of different structural forms. In the larger basis set, STO-3G is replaced by 6-31G.

All calculations were performed using the Gaussian 98 software package.<sup>56</sup> Natural bond orbital (NBO) analysis was performed by using the NBO program<sup>57</sup> to evaluate the  $\pi$ -accepting ability of boryl ligands.

**Acknowledgment.** S.S. thanks the Science and Technology Agency of Japan for a fellowship and Dr. M. Tanaka for granting sabbatical leave, making possible his stay in Durham. Z.L. thanks the Research Grants Council of Hong Kong for financial support. T.B.M. thanks the EPSRC (U.K.) for research support, the Leverhulme Trust for a Study Abroad Fellowship, the Hong Kong University of Science and Technology for a Visiting Professorship, and the University of

Durham for granting research leave, making possible his stay in Hong Kong. J.A.K.H. thanks the EPSRC for a Senior Research Fellowship. J.A.C. thanks the EPSRC and ILL for studentship support.

**Supporting Information Available:** Listings of the structural parameters for **3Bcat** and **3Bpin** derived from both X-ray and neutron diffraction data. This material is available free of charge via the Internet at <http://pubs.acs.org>.

OM030434D

(55) (a) Hehre, W. J.; Stewart, R. F.; Pople, J. A. *J. Chem. Phys.* **1969**, *51*, 2657–2664. (b) Collins, J. B.; Schleyer, P. v. R.; Binkley, J. S.; Pople, J. A. *J. Chem. Phys.* **1976**, *64*, 5142–5151.

(56) Frisch, M. J.; Trucks, G. W.; Schlegel, H. B.; Scuseria, G. E.; Robb, M. A.; Cheeseman, J. R.; Zakrzewski, V. G.; Montgomery, J. A., Jr.; Stratmann, R. E.; Burant, J. C.; Dapprich, S.; Millam, J. M.; Daniels, A. D.; Kudin, K. N.; Strain, M. C.; Farkas, O.; Tomasi, J.; Barone, V.; Cossi, M.; Cammi, R.; Mennucci, B.; Pomelli, C.; Adamo, C.; Clifford, S.; Ochterski, J.; Petersson, G. A.; Ayala, P. Y.; Cui, Q.; Morokuma, K.; Malick, D. K.; Rabuck, A. D.; Raghavachari, K.; Foresman, J. B.; Cioslowski, J.; Ortiz, J. V.; Stefanov, B. B.; Liu, G.; Liashenko, A.; Piskorz, P.; Komaromi, I.; Gomperts, R.; Martin, R. L.; Fox, D. J.; Keith, T.; Al-Laham, M. A.; Peng, C. Y.; Nanayakkara, A.; Gonzalez, C.; Challacombe, M.; Gill, P. M. W.; Johnson, B. G.; Chen, W.; Wong, M. W.; Andres, J. L.; Head-Gordon, M.; Replogle, E. S.; Pople, J. A. *Gaussian 98*, revision A.9; Gaussian, Inc.: Pittsburgh, PA, 1998.

(57) Glendening, E. D.; Reed, A. E.; Carpenter, J. E.; Weinhold, F. *NBO*, version 3.1.

(54) (a) Gordon, M. S. *Chem. Phys. Lett.* **1980**, *76*, 163–168. (b) Hariharan, P. C.; Pople, J. A. *Theor. Chim. Acta* **1973**, *28*, 213–222. (c) Binning, R. C., Jr.; Curtiss, L. A. *J. Comput. Chem.* **1990**, *11*, 1206–1216.